Ultra-thin Co/Pd multilayers with enhanced high-temperature annealing stability

M. Gottwald,[1] K. Lee,[2] J. J. Kan,[1] B. Ocker,[3] J. Wrona,[3] S. Tibus,[3] J. Langer,[3] S. H. Kang,[2] and E. E. Fullerton[1]
[1]*Center for Magnetic Recording Research, University of California, San Diego, La Jolla, California 92093-0401, USA*
[2]*Advanced Technology, Qualcomm Incorporated, San Diego, California 92121-1714, USA*
[3]*Singulus Technologies AG, Hanauer Landstrasse 103, D-63796 Kahl am Main, Germany*

(Received 14 November 2012; accepted 28 January 2013; published online 6 February 2013)

Understanding the thermal budget of perpendicular materials is crucial for the potential application perpendicular magnetic tunnel junctions. In this paper, we study the effects of high-temperature rapid thermal annealing on the structural and magnetic properties of ultra-thin Co/Pd multilayers deposited at room temperature. It is shown that perpendicular magnetic anisotropy of ultra-thin Co/Pd multilayers improves with increasing annealing temperature up to 425 °C. This property of ultra-thin Co/Pd multilayers provides increased thermal budgets for CMOS-integrated magnetic devices. © *2013 American Institute of Physics*. [http://dx.doi.org/10.1063/1.4791577]

The thermal budget of magnetic tunnel junctions (MTJs) has been an important subject for integrating magnetic devices into a complementary metal-oxide-semiconductor (CMOS) platform.[1–4] Thermal cycles required for CMOS back-end-of-line (BEOL) can affect the magnetic properties of MTJs via atomic interdiffusion and phase change. This challenge has been particularly important for embedded spin-transfer-torque magneto-resistive random access memory (STT-MRAM) because it is preferred to integrate a MTJ module into a pre-established CMOS logic platform with minimal modification of BEOL processes that may involve short high-temperature thermal cycles.

While in-plane MTJs have been integrated into a 45-nm CMOS logic platform,[5] the thermal budget poses a greater challenge for perpendicular MTJs (pMTJs), limiting material options available for pMTJ film stacks. For example, the perpendicular magnetic anisotropy (PMA) of Co/Ni multilayers disappears upon high-temperature annealing above 350 °C.[6] TbFeCo is not thermally stable even above 200 °C.[7] Therefore, understanding the thermal budget of perpendicular materials is crucial for optimizing pMTJ film stacks.

There have been a number of reports on pMTJ film stacks using various perpendicular materials, including $L1_0$-ordered FePt,[8] CoFe/Pd,[9,10] Co/Pd,[11–13] and Co/Pt.[14,15] While $L1_0$-ordered FePt provides strong crystalline anisotropy and is compatible with high temperature annealing,[8] the $L1_0$ phase ordering temperature of FePt is typically above 400 °C, requiring high-temperature deposition.[16] Also, the grain size of FePt and surface roughness may need to be decreased for deeply scaled pMTJs, which has also been a significant challenge for perpendicular recording media.[17] On the other hand, Co-based multilayers can be easily grown by standard sputtering deposition techniques and their magnetic properties can be tuned by changing thickness and number of repeats. However, the PMA of co-based multilayers is known to degrade upon high-temperature annealing.[18]

In this work, we present enhanced high-temperature annealing stability of ultra-thin Co/Pd multilayers. The Co/Pd multilayers retained PMA upon rapid thermal annealing (RTA) at 425 °C. Furthermore, RTA improves the PMA field (H_K) and squareness up to 425 °C. This is surprising because high-temperature annealing usually degrades the PMA of such thin multilayers due to atomic interdiffusion.[19] It is speculated that the ultra-thin Co/Pd multilayers deposited at room temperature formed an ordered-alloy-like structure and RTA improved the ordering of the Co/Pd multilayers, enhancing PMA with increasing annealing temperatures.

The Co/Pd multilayers studied were deposited at room temperature by DC sputtering (Singulus 300 mm TIMARIS tool). The magnetic properties of the films before and after RTA were examined by vibrating sample magnetometry (VSM). The sample structure, texture, and surface roughness were analyzed by atomic force microscopy (AFM) and X-ray diffraction (XRD). To examine the effect of Pd layer thickness (t_{Pd}), we utilized the wedge film deposition technique for Pd layers. The film stack was substrate/bottom electrode/seed layers/$[Co(0.2)/Pd(0.17–0.62)]_{x6}$/Pd(3) (thickness in nm). The Pd wedge thickness was pre-calibrated on 6-in. wafers. The thickness range of the Pd wedge was 0.17–0.34 nm for the first wafer and 0.32–0.62 nm for the second wafer. The deposition power for Pd wedge layers was adjusted (low power) for accurate wedge thickness control. The bottom electrode was a Ta/CuN multilayers and seed layers were Ta/Ru. In addition, Co/Pd multilayers with fixed Pd thickness of 0.2 nm, $[Co(0.2)/Pd(0.2)]_{x6}$, were also grown on top of optimized bottom electrode/seed layers. The Pd deposition power was increased for this non-wedge film.

AFM images (Fig. 1(a)) of as-grown samples show a smooth sample surface. The height variations along the AFM tip scans are typically below 0.5 nm (Fig. 1(b)). A roughness analysis of the height distribution (Fig. 1(c)) resulted in RMS surface roughness of 0.17 nm. The X-ray reflectivity diffraction (XRD) Θ-2Θscans (Fig. 1(d)) show the presence of hexagonal-close-packed (hcp)-Ru (0002), face-centered-cubic fcc-Cu(111), and fcc-Cu (200). It is noteworthy that satellite peaks appear next to the primary Ru(0002) peak, which result

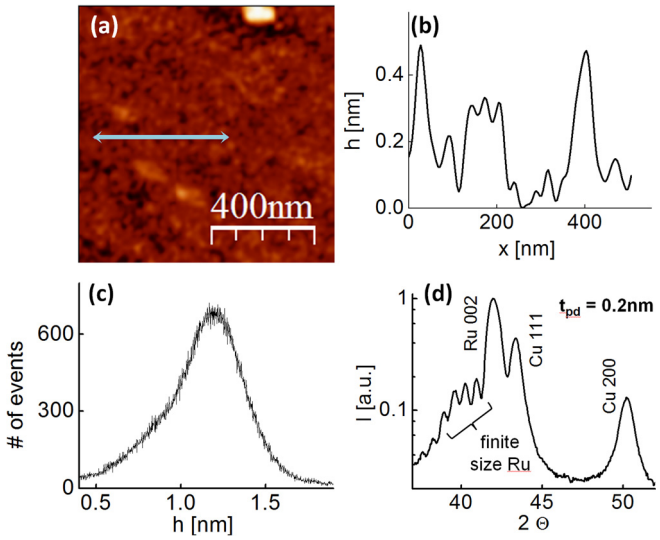

FIG. 1. [Co (0.2)/Pd (0.2)]$_{x6}$ sample: (a) AFM image of the sample surface (b) Arbitrary profile of the AFM picture along scanning direction. (c) Roughness analysis showing the height distribution of the AFM image. (d) XRD 2Θ scan.

from finite-size effects from the 10-nm-thick Ru seed layer. The separation of the peaks gives a layer thickness of 12 nm. This indicates that Ru seed layer is very smooth, and crystalline coherence is maintained through the thickness. For comparable Co/Pd multilayer films deposited on the bottom electrode with increased surface roughness, such satellite peaks did not show up and significantly smaller PMA was observed. We hence conclude that low surface roughness and high crystalline quality of the Ru seed is critical for achieving high-quality ultra-thin Co/Pd multilayers. Also, note that the hcp (0002) texture of Ru works as a starting template for the fcc (111) Co/Pd layers.[20]

Figure 2 summarizes the effects of annealing on the magnetic properties as a function of the Pd-thickness t_{Pd}. Two annealing conditions were studied: 1 h 300 °C vacuum annealing and 12 min RTA under N_2 atmosphere at higher

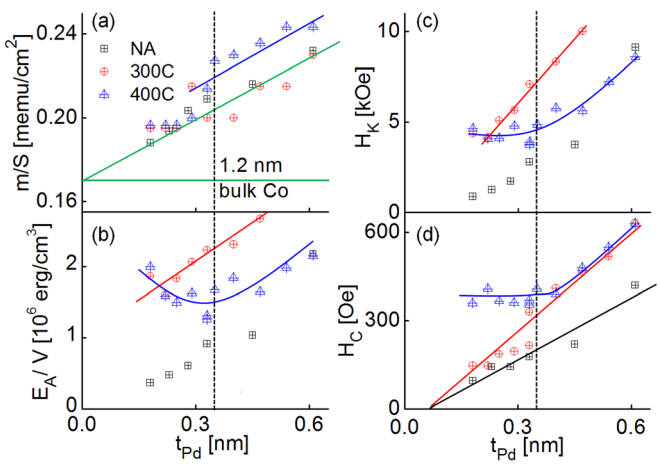

FIG. 2. Annealing behavior of [Co (0.2)/Pd(t)]$_{x6}$ (thickness in nm) multilayers deposited on optimized seed layers. NA: not annealed, 300 °C: 1h vacuum annealing, 400 °C: 12 min rapid thermal annealing under N_2 atmosphere at 400 °C. All lines are guides to the eye. (a) Moment per surface m/S, (b) coercivity H_C, (c) anisotropy field H_K, and (d) anisotropy energy density E_A/V as a function of Pd thickness t_{Pd}.

temperatures. Coercivity (H_C) and magnetic moment were extracted from out-of-plane magnetization loops. H_K was calculated by integrating VSM hysteresis loops where the field was applied in the sample plane. Figure 2(a) shows that the magnetic moment per cm^2 increases with thicker Pd layers. This is because Pd gets magnetically polarized by adjacent Co layers and contributes to the magnetic moment of the Co/Pd multilayers.[21] For both as-grown and magnetic-annealed samples, H_C and H_K increased with increasing t_{Pd} as shown in Figs. 2(c) and 2(d). However, for samples exposed to 400 °C RTA, H_C and H_K are nearly constant when t_{Pd} is less than 0.35 nm. This resulted in increased anisotropy energy (E_A) per volume with decreasing t_{Pd} (Fig. 2(b)). It has been known that the PMA of fcc(111)-textured Co/Pd multilayers originates from at least two sources. First, the (0001) hcp direction of fcc Co is an easy axis of the magnetocrystalline anisotropy of Co. However, this magnetocrystalline anisotropy of Co is not enough to overcome the thin-film shape anisotropy. Therefore, there has to be additional source of anisotropy, which is discussed in literatures as Co/Pd interface anisotropy, magnetostriction and interface alloy formation.[22,23] However, this result indicates that the origin of PMA in the Co/Pd multilayers may be different when $t_{Pd} < 0.35$ nm than for thicker layers. Yakushiji *et al.*[14] reported that smooth ultra-thin Co/Pd or Co/Pt multilayers deposited at 250 °C can form an ordered-alloy-like structure with fcc(111) orientation in which atomic interdiffusion is suppressed. These films were also stable against annealing up to 370 °C. It is speculated that the different regime shown at $t_{pd} < 0.35$ nm is due to the presence of such an ordered-alloy-like structure.

To further optimize ultra-thin Co/Pd multilayers, we fixed the Pd thickness to 0.2 nm and examined the effect of Pd deposition power on the annealing stability. Figure 3 shows magnetization loops of [Co(0.2)/Pd(0.2)]$_{x6}$ deposited at two different Pd deposition powers, 87 mW/cm^2 and 290 mW/cm^2. The Co/Pd multilayers with lower Pd deposition power (low-P sample) showed PMA in the as-deposited state (Figs. 3(a) and 3(d)) whereas the as-grown samples with higher Pd deposition power (high-P sample) exhibited in-plane anisotropy (Figs. 3(b) and 3(e)). For both cases, annealing increased PMA, resulting in fully perpendicular magnetization ($H_K = 6.2$ kOe) of the high-P sample upon 12 min RTA at 400 °C. For the low-P sample, H_K was 4.8 kOe after applying the same RTA condition. We speculate that lower Pd deposition power leads to higher crystalline texture and, therefore, higher anisotropy in the as-grown state. However after RTA, the high-P sample shows higher PMA. This indicates that the improvement of the sample structure by RTA does not depend on the as-grown state. It has been known that faster growth allows less inclusion of impurities like Ar atoms into the deposited films,[18] which may explain higher PMA observed in the high-P sample after RTA. To investigate the effect of RTA temperatures, 5 high-P samples from the same wafer were treated by 12 min RTA at various temperatures (360 ~ 450 °C). Figure 4(b) shows that H_K slightly increases from 5.1 kOe to 6.3 kOe as the annealing temperature increased from 360 to 425 °C. The out-of-plane magnetization hysteresis loops show 100% remanence in the temperature range (Fig. 4(a)). H_C remains constant (~350 Oe) over temperatures. However after 450 °C

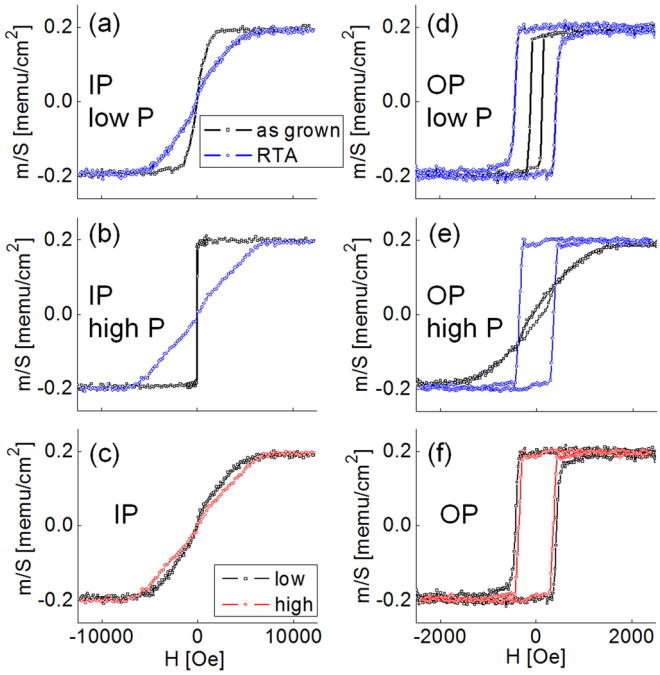

FIG. 3. Influence of Pd deposition power on the properties of ultrathin $[Co0.2/Pd0.2]_{x6}$ multilayers. Low power $P = 87\,mW/cm^2$ (low P), high power $P = 290\,mW/cm^2$ (high P). Compared are the hysteresis loops for as-grown samples and samples exposed to 12 min RTA at 400 °C under N_2 atmosphere. In-plane hysteresis loops (IP) for low Pd deposition power are shown in (a) and for high Pd deposition power in (b). Out of plane hysteresis loops for low Pd deposition power are shown in (d) and for high Pd deposition power in (e). (c) and (f) compare in plane (IP) and out of plane (OP) loops after 12 min RTA at 400 °C for high and low deposition power.

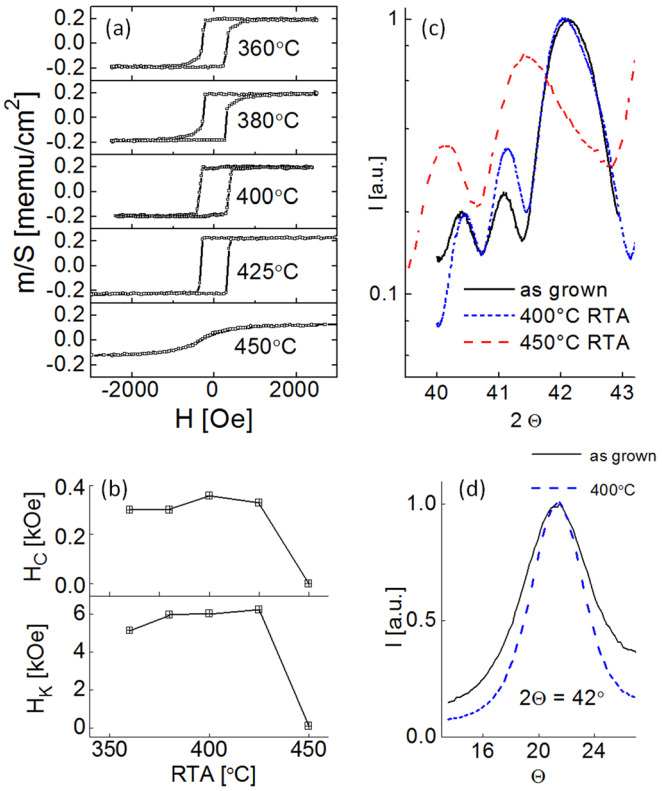

FIG. 4. Rapid thermal annealing behavior of a $[Co0.2/Pd0.2]_{x6}$ multilayer: All annealing done under N_2 atmosphere during 12 min. (a) Out of plane VSM hysteresis loops for different annealing temperatures. (b) Coercivity H_C and anisotropy field H_K as a function of RTA temperature. (c) XRD 2Θ scans (d) Rocking curve of the Ru (002) hcp peak before and after annealing.

RTA, PMA completely disappeared along with the magnetic moment decreased by a factor of two.

Figure 4(d) shows the rocking curve of Ru (0002) peak before and after 400 °C RTA. The rocking curve width decreased from 6.5° to 4.8°, which implies that the texture of the overall structure, including the Co/Pd layers improves. It has also been reported that the enhanced PMA of Co/Pd multilayers upon annealing can be attributed to improved texture and sharpening of the Co/Pd interfaces.[17] Hence enhanced H_K with increasing RTA temperatures seems to be related to the improved texture. However, it is still unusual that the PMA is not degraded through intermixing of only 0.2 nm thick Co and Pd layers even at 425 °C. As mentioned earlier, the ordered-alloy-like structure seems to suppress randomizing of Co and Pd atoms, allowing texture improvement with increasing annealing temperatures. Figure 4(c) shows XRD 2Θ scans before and after RTA. For the samples either in the as-deposited state or annealed at 400 °C, a Ru (002) peak at 42° is observed. However, the sample annealed at 450 °C shows a broader peak with a maximum around 41.5°, indicating a change of the sample structure. This peak is probably due to an alloy of the Ru seed with the Co/Pd multilayer. This would also explain the substantial reduction of magnetic moment after 450 °C RTA.

In summary, we have shown that ultra-thin Co/Pd multilayers deposited at room temperature by DC sputtering can retain PMA for RTA up to 425 °C. The results are very promising for applications involving CMOS BEOL processing as this materials class provides additional thermal budget margins. It is believed that the ultrathin Co/Pd multilayers form an ordered-alloy-like structure with improved texture rather than multilayers with individual films separated. In this case, high-temperature annealing enhances the texture and chemical order and thereby PMA with the atomic inter-diffusion being suppressed. As a result, it was observed that the PMA of the ultrathin Co/Pd multilayers increased with increasing annealing temperature. AFM and XRD data revealed that atomically flat seed layers are essential to achieve enhanced high-temperature annealing stability from ultrathin Co/Pd multilayers. With film deposition conditions fully optimized, it is expected that the PMA of Co/Pd multilayers can be improved further while retaining the high-temperature annealing stability.

[1]K. Sutemitsu, Y. Kawano, H. Utsumi, H. Honjo, R. Nebashi, S. Saito, N. Ohshima, T. Sugibayashi, H. Hada, T. Nohisa, T. Shimazu, M. Inoue, and N. Kasai, Jpn. J. Appl. Phys., Part 1 **47**, 2714 (2008).
[2]Y. Fukumoto, K. Shimura, A. Kamijo, S. Tahara, and H. Yoda, Appl. Phys. Lett. **84**, 233 (2004).
[3]S. V. Pietambaram, J. Janesky, R. W. Dave, J. J. Sun, G. Steiner, and J. M. Slaughter, IEEE Trans. Magn. **40**, 2619 (2004).
[4]K. Kinoshita, in *Proceedings of the 21st edition of the Great Lakes Symposium on VLSI* (2011), pp. 445–446.
[5]C. J. Lin, S. H. Kang, Y. J. Wang, K. Lee, X. Zhu, W. C. Chen, X. Li, W. N. Hsu, Y. C. Kao, M. T. Liu, Y. C. Lin, M. Nowak, N. Yu, and L. Tran, IEDM Tech. Dig. **2009**, 1–4.
[6]H. Kurt, M. Venkatesan, and J. M. D. Coey, J. Appl. Phys. **108**, 073916 (2010).
[7]Z. G. Li, D. J. Smith, E. E. Marinero, and J. A. Willett, J. Appl. Phys. **69**, 6590 (1991).

[8]M. Yoshikawa, E. Kitagawa, T. Nagase, T. Daibou, M. Nagamine, K. Nishiyama, T. Kishi, and H. Yoda, IEEE Trans. Magn. **44**(11), 2573 (2008).
[9]K. Mizunuma, S. Ikeda, H. Sato, M. Yamanouchi, H. D. Gan, K. Miura, H. Yamamoto, J. Hayakawa, F. Matsukura, and H. Ohno, J. Appl. Phys. **109**, 07C711 (2011).
[10]K. Mizunuma, S. Ikeda, J. H. Park, H. Yamamoto, H. Gan, K. Miura, H. Hasegawa, J. Hayakawa, F. Matsukura, and H. Ohno, Appl. Phys. Lett. **95**, 232516 (2009).
[11]M. T. Rahman, A. Lyle, G. Hu, W. J. Gallagher, and J.-P. Wang, J. Appl. Phys. **109**, 07C709 (2011).
[12]Z. R. Tadisina, A. Natarajarathinam, B. D. Clark, A. L. Highsmith, T. Mewes, S. Gupta, E. Chen, and S. Wang; J. Appl. Phys. **107**, 09C703 (2010).
[13]D. C. Worledge, G. Hu, D. W. Abraham, J. Z. Sun, P. L. Trouilloud, J. Nowak, S. Brown, M. C. Gaidis, E. J. O'Sullivan, and R. P. Robertazzi, Appl. Phys. Lett. **98**, 022501 (2011).
[14]K. Yakushiji, T. Saruya, H. Kubota, A. Fukushima, T. Nagahama, S. Yuasa, and K. Ando, Appl. Phys. Lett. **97**, 232508 (2010).
[15]K. Machida, K. Furukawa, T. Nakayama, N. Funabashi, K. Aoshima, K. Kuga, H. Kikuchi, T. Ishibashiand, and N. Shimidzu, J. Phys.: Conf. Ser. **303**, 012100 (2011).
[16]M. Weisheit, L. Schultz, and S. Fähler, Thin Solid Films **515**, 3952–3955 (2007).
[17]R. Sbiaa, H. Meng, and S. N. Piramanayagam, Phys. Status Solidi RRL **5**(12), 413–419 (2011).
[18]H. Yamane, Y. Maeno, and M. Kobayashi, J. Appl. Phys. **73**(I), 334 (1993).
[19]M. T. Johnson, P. J. H. Bloemen, F. J. A. den Broeder, and J. J. de Vries, Rep. Prog. Phys. **59**, 1409 (1996).
[20]A. Dinia, K. Ounadjela, A. Arbaoui, G. Suran, D. Muller, and P. Panissod, J. Magn. Magn. Mater. **104–107**(3), 1871–1872 (1992).
[21]D. G. Stinson and S.-C. Shin, J. Appl. Phys. **67**, 4459 (1990).
[22]B. N. Engel, C. D. England, R. A. Van Leeuwen, M. H. Wiedmann, and C. M. Falco, Phys. Rev. Lett. **67**(14), 1910 (1991).
[23]J. M. Shaw, H. T. Nembach, T. J. Silva, S. E. Russek, R. Geiss, C. Jones, N. Clark, T. Leo, and D. J. Smith; Phys. Rev. B **80**, 184419 (2009).